Structure of low-lying states in ^{116}Te

F. von Spee ®,* M. Beckers, A. Blazhev ®, A. Dewald, F. Dunkel, A. Esmaylzadeh, C. Fransen ®, G. Hackenberg, J. Jolie ®, L. Knafla ®, C.-D. Lakenbrink ®, M. Schiffer, N. Warr ®, and M. Weinert ®

Institut für Kernphysik, Universität zu Köln, Zülpicher Straße 77, 50937 Köln, Germany

Low-lying excited levels in ^{116}Te were studied by measuring level lifetimes with the recoil-distance Doppler-shift method in the ^{112}Sn(^{12}C, ^{8}Be) ^{116}Te α-transfer reaction and angular correlations following the β decay of ^{116}I. Both experiments were performed at the Cologne FN Tandem accelerator. Several new levels were discovered below 3.2 MeV excitation energy, spins and multipole mixing ratios were determined via angular correlations. Lifetimes were measured for the $2_1^+, 0_2^+, 2_2^+,$ and 4_1^+ and upper limits for lifetimes were determined for higher lying levels. The experimental findings are compared to calculations in the U(5) limit of the interacting boson model and are also discussed in the framework of shape coexistence which is expected in midshell Te isotopes.

I. INTRODUCTION

The low-lying level structure of midshell Te isotopes resembles that of a vibrational nucleus in a similar fashion to the midshell Cd isotopes, that mirror the Te isotopes with respect to the $Z = 50$ proton shell closure. In the Cd isotopes it is well known that this vibrational picture is not sufficient to describe the low lying structure and that instead many observables indicate that shape coexistence is needed to understand the low-lying structure of midshell Cd isotopes [1]. Additional 0^+ and 2^+ states were found [2] close to the $0_2^+, 2_2^+,$ and 4_1^+ states that were presumed to be the two phonon triplet. These states were in some cases strongly populated in the (^{3}He, n) transfer reaction [3]. This can be an indication that these states belong to 2p-4h intruder structures [1]. Band structures were found on top of excited 0^+ states [4], also with the help of $B(E2)$ strengths of the in-band transitions [5]. Experimental signatures of shape coexistence in the Cd isotopes are well summarized for example in Refs. [1,6].

Since the Te isotopes mirror the Cd isotopes with respect to the $Z = 50$ proton shell closure, the discovery of shape coexistence in midshell Cd isotopes has lead to the suspicion that shape coexistence is also present in midshell Te isotopes. Over 30 years ago, Rikovska *et al.* identified intruder states using existing level systematics and relative $B(E2)$ values [7]. As of today, experimental evidence for shape coexistence in Te, however, is still not nearly as clear as it is in the Cd isotopes. The $B(E2, 4_1^+ \rightarrow 2_1^+)/B(E2, 2_1^+ \rightarrow 0_1^+)$ ($B_{4/2}$) ratios are inconsistent along the isotopic chain: in ^{118}Te a $B_{4/2}$ ratio of 2.1(6) was measured by Pasternak *et al.* [8] in agreement with a vibrational picture while Möller *et al.* measured a $B_{4/2}$ ratio of 0.84(14) in ^{114}Te that cannot be explained by any collective model [9]. From a second lifetime measurement in ^{118}Te the absolute transition strength $B(E2, 2_3^+ \rightarrow 0_2^+) = 60_{-17}^{+30}$ W.u. [10] was measured. This

value could indicate that the 2_3^+ state is indeed a first member of an intruder band built on top of the 0_2^+ state. For most other suspected intruding structures in midshell Te, possible in-band transitions have not yet been observed or absolute transition strengths are missing. The status quo of experimental evidence for shape coexistence in Te isotopes—or the absence of such experimental evidence—is well summarized in [1].

For ^{116}Te, experimental data are especially scarce. Here, any data analysis of γ rays is particularly challenging, since the $4_1^+ \rightarrow 2_1^+$ and $2_1^+ \rightarrow 0_1^+$ transitions lie less than 2 keV apart at 680.8 and 678.9 keV [11]. The two more extensive studies focusing on the low-lying structure of ^{116}Te are a decay study performed by Zimmerman [12] and an in-beam experiment using a (^{3}He, $3n$) reaction performed by Lönnroth *et al.* [13]. These studies were able to identify a couple of low-lying off-yrast states, but data seem incomplete and partially contradict each other. Other experiments have been focusing more on high-spin states [14–17] and only provide limited insight into the low-lying level structure. Data on absolute transition strengths have not been published up to now.

It is the aim of this study to investigate the low-lying structure in ^{116}Te and measure lifetimes of low-lying excited states. For this purpose, low-lying states in ^{116}Te were populated in two different experiments using the ^{112}Sn(^{12}C, ^{8}Be) ^{116}Te α-transfer reaction and β decay from ^{116}I. From these two data sets, the level scheme was extended and spins and parities were assigned with the help of γ-γ angular correlations. Absolute transition strengths were extracted, using the obtained lifetime values, branching ratios, and multipole mixing ratios. The new experimental data help to improve the understanding of the low-lying level structure.

II. EXPERIMENT

To analyze the low-lying structure in ^{116}Te, two experiments were performed at the FN tandem accelerator

---

*fspee@ikp.uni-koeln.de

in Cologne. In a first experiment with the recoil-distance Doppler-shift (RDDS) technique, the nucleus was produced in an α-transfer reaction ^{112}Sn(^{12}C, ^{8}Be)^{116}Te with a beam energy of 44 MeV. The target foil was 0.3 mg/cm^2 ^{112}Sn on a 1.4 mg/cm^2 Ta fronting. The ^{112}Sn target material was 80% isotopically enriched. The stopper was a 5 mg/cm^2 Ta foil. The foils were mounted inside the Cologne Plunger device [18] and nine different target-to-stopper distances between 9 and 509 μm were measured. The target-to-stopper distance was monitored during the experiment using the capacitance method introduced by Alexander and Bell [19]. Eleven high-purity Germanium (HPGe) detectors were placed at angles of 45° and 142° with respect to the beam axis to observe Doppler-shifted and unshifted γ rays. The relative efficiency of the HPGe detectors varied between 55% and 90%. Four PIN diodes ("solar cells") were mounted at backwards angles between 120° and 160° to detect α particles stemming from the decay of ^{8}Be. The solar cells were covered with a 40 μm aluminum foil to prevent heavier beam-like fragments, e.g., ^{12}C, ^{10}Be, from entering into the solar cells. Data were collected triggerless for about 16 h for each target-to-stopper distance.

In a second experiment, ^{116}Te was populated in the β decay of ^{116}I with a half-life of 2.9 s. The reaction ^{107}Ag(^{12}C, 3n)^{116}I with a beam energy of 52 MeV was used to produce ^{116}I. The products of fusion-evaporation reactions were stopped in the 10 mg/cm^2 thick ^{107}Ag target. In this experiment, a pulsed beam was used where the times of beam-on and beam-off were 5 s each. The HORUS spectrometer [20] was used to detect γ rays following the β decay of reaction products. Data were again collected triggerless for about 24 h.

III. ANALYSIS

The data of the α-transfer experiment were sorted into particle-γ and particle-γ-γ matrices. In total, 10^7 particle-γ events were collected. A Doppler correction was performed using the average recoil velocity of the nuclei after leaving the target and differentiating between different solar-cell-Germanium pairs. Doppler-corrected spectra were used to identify shorter lived, weakly populated transitions and measure their intensities. For the RDDS analysis, noncorrected spectra were used. The average ^{116}Te recoil velocity was determined to be 1.1(1) % c. The measured particle spectrum is shown in Fig. 1. Protons from fusion-evaporation reactions can be found below channel 700, α particles can be found throughout the whole spectrum. At around channel 600, a structure can be seen that is introduced by the feedback system of the plunger device. The feedback system is implemented as described in Ref. [18] and uses a pulse signal for the capacitance measurement. The pulse signal of the plunger feedback system couples with the solar cells and introduces a signal, that can be observed in the solar-cell spectra. The pulse signal was chosen in a way, that the signal induced in the solar cells lies outside of the gate region used for the analysis. A gate onto energies above channel 700 allows to select only events stemming from α-transfer reactions. Figure 2 shows the Doppler-corrected coincidence spectrum of the indicated gate, with the statistics of all detectors and target-to-stopper
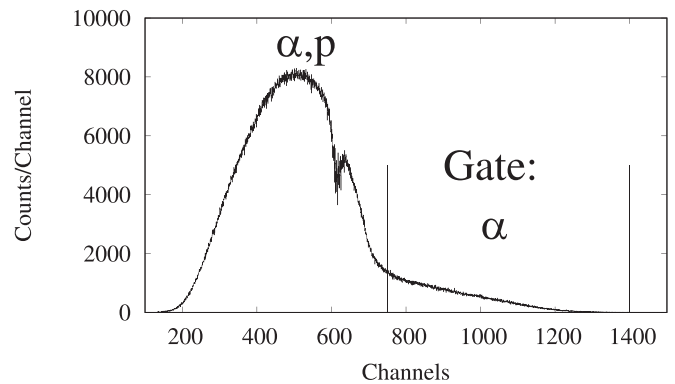

FIG. 1. Particle spectrum observed by the solar cells. Protons from fusion-evaporation reactions like ^{112}Sn(^{12}C, np)^{122}Cs, ^{112}Sn(^{12}C, 2p)^{122}Xe were found at energies below channel 700. The gate was set for higher energies, to select only α particles. The corresponding coincident spectrum in the HPGe detectors is show in Fig. 2. The structure at around channel 600 is introduced by the electronics of the Plunger device.

distances summed. The intensities of lines belonging to transitions in ^{116}Te are shown in Table I.

Data of the β-decay experiment were sorted into γ-γ matrices. In this experiment, 2×10^{10} γ-γ events were recorded. In the ^{107}Ag(^{12}C, X)Y reaction, many different nuclei between ^{116}I and ^{110}Sb were populated. In the data that were collected off-beam, γ rays from consequent β decays were detected. To clean the data, γ-γ coincidences were used. A spectrum in coincidence with the $2_1^+ \rightarrow 0_1^+$ transition (679 keV) in ^{116}Te can be seen in Fig. 3. The intensities of lines belonging to transitions in ^{116}Te populated in the β decay of ^{116}I are shown in Table II.

A. Angular correlation analysis

The cube geometry of the HORUS spectrometer leads to six different angles between pairs of detectors (angular groups) at 55°, 70°, 90°, 110°, 125°, and 180°.

TABLE I. All observed γ-ray transitions in ^{116}Te from the α-transfer reaction. Intensities are given relative to the 680 keV doublet since it is the most precisely determined intensity. The uncertainties of the intensities of the $4_1^+ \rightarrow 2_1^+$ transition (681 keV) and the $2_1^+ \rightarrow 0_1^+$ transition (679 keV) are correlated. The uncertainties on the measured transition energies are only given for those γ rays that are newly observed and if the transition energy could not be determined through known level energies.

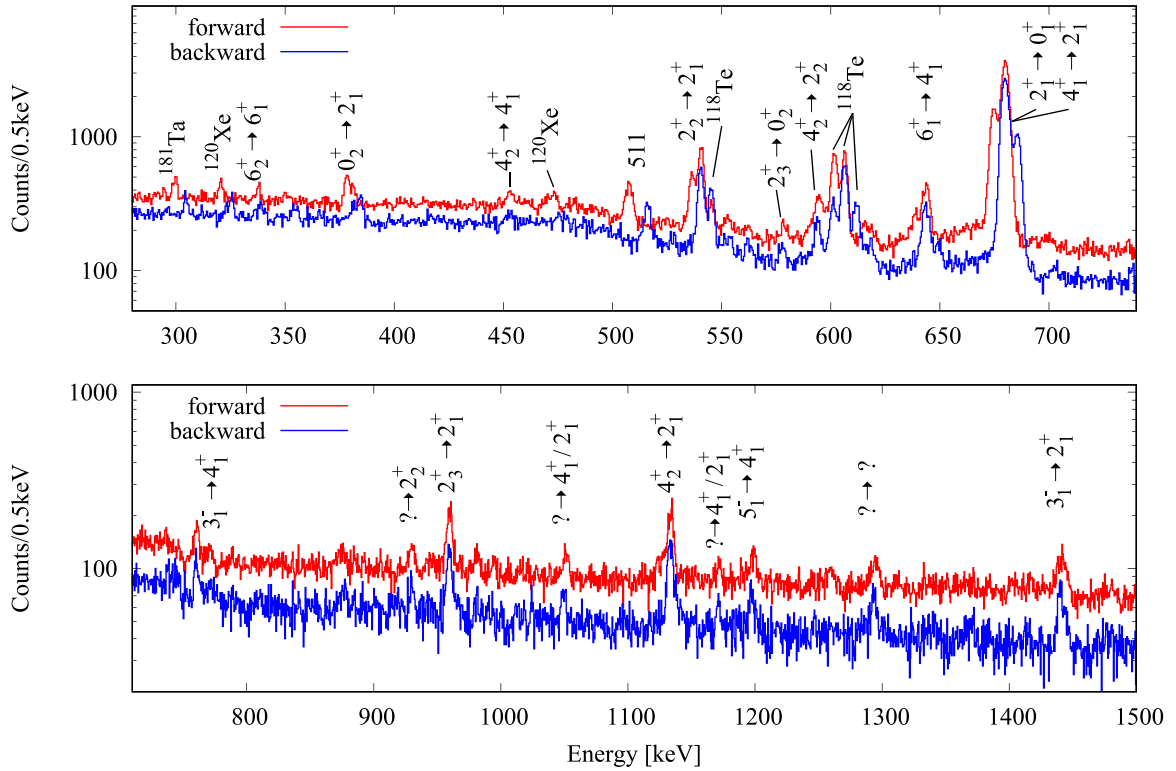| E_γ [keV]	Intensity	E_γ [keV]	Intensity	E_γ [keV]	Intensity
338	0.82(9)	679	68(3)	1133	6.0(2)
381	2.69(13)	681	32(3)	1171(2)	0.63(10)
540	10.9(3)	760	1.4(2)	1198	1.8(2)
453	0.86(12)	930(2)	1.08(10)	1294(2)	1.9(2)
578	0.66(9)	959	3.7(2)	1441	3.0(2)
594	2.7(3)	981	0.68(9)	1588	1.1(2)
643	5.3(3)	1050(2)	0.94(13)	1902	1.6(2)

FIG. 2. Doppler-corrected γ-ray spectrum obtained in coincidence with solar cells in the α-transfer experiment. All target-to-stopper distances are summed for the full statistics. An artificial vertical offset of 40 counts has been added to the spectrum of the detectors at forward angle to make the figure more illustrative. Note that the Doppler correction leads to a broadening of the stopped component and a narrowing of the flight component. The flight component is on the nominal energy and the stopped component is shifted. Transitions in ^{116}Te are denoted by spin and parity of the initial and final state, states with unknown spin and parity are denoted with a question mark. Contaminating transitions—stemming from, e.g., target impurities—are denoted by the nucleus in which they take place.

These angular groups were used to perform a γ-γ angular correlation analysis of the data gathered in the β-decay experiment. The angular groups were normalized by the number of detectors and efficiency corrected using the event mixing approach as described in [21,22]. Standard corrections of random coincidences and Compton background were applied. The measured angular dependent intensities were then fitted using the angular correlation probability distribution:

$$W(\theta) = A_0 \left[1 + \sum_{k=2,4} q_k a_k P_k(\cos\theta) \right], \qquad (1)$$

where P_k are Legendre polynomials, a_k are the angular correlation coefficients. A detailed introduction to the theory of angular correlations can be found in Ref. [23]. The

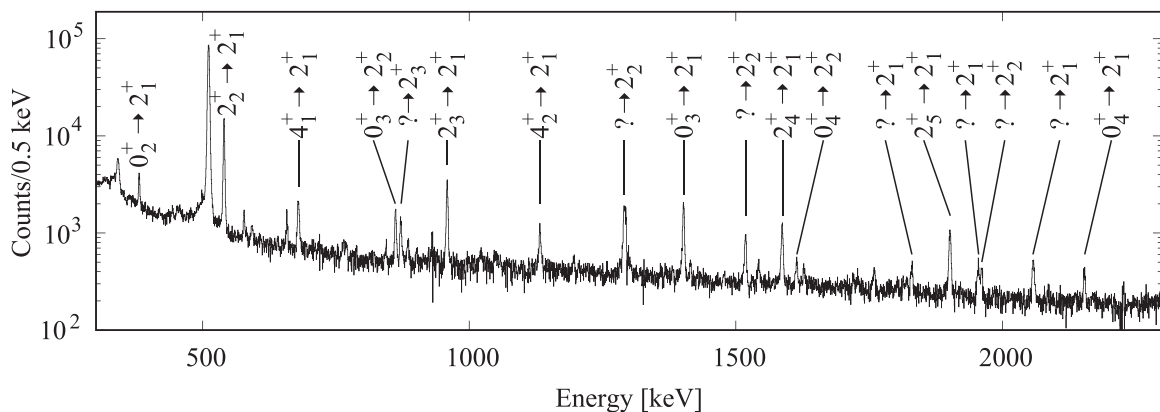FIG. 3. Spectrum showing γ rays in coincidence with the 679 keV transition in ^{116}Te observed in the β-decay experiment. The statistics of all detectors were summed for this figure. Note that for illustrative purposes not all visible γ rays were marked.

TABLE II. All γ-ray transitions in ^{116}Te observed in the β-decay experiment. Percentage intensities are given relative to the 679 keV transition.

E_γ [keV]	Intensity	E_γ [keV]	Intensity	E_γ [keV]	Intensity
380.9(1)	1.04(10)	871.3(2)	1.06(10)	1628.0(5)	0.27(3)
419(1)	$\leqslant 0.1$	958.5(2)	3.8(3)	1728.7(6)	0.25(3)
443(1)	$\leqslant 0.2$	1132.4(3)	1.16(10)	1759.4(7)	0.51(6)
452(1)	$\leqslant 0.25$	1195.6(4)	0.25(3)	1829.9(6)	0.49(5)
539.9(1)	9.8(4)	1290.0(5)	2.7(4)	1901.6(4)	1.8(2)
577.6(1)	0.5(1)	1401.7(4)	2.9(2)	1954.7(5)	0.61(6)
592.5(2)	0.26(3)	1414.7(4)	0.26(3)	1961.4(4)	0.63(10)
678.8(1)	100	1517.9(4)	1.40(10)	2057.7(5)	0.92(10)
680.6(3)	0.7(2)	1542.7(5)	0.34(4)	2153.8(6)	0.6(1)
769(1)	0.2(1)	1586.8(5)	1.8(2)	2736(1)	1.0(2)
861.8(1)	1.41(15)	1614.1(5)	0.47(5)		

attenuation coefficients q_k were geometrically determined to be $q_2 = 0.95(1)$ and $q_4 = 0.85(1)$. It turned out that only cascades containing the ground state transition $2_1^+ \to 0_1^+$ (679 keV) had enough statistics to be used in this analysis. At first, a free fit of the parameters a_2 and a_4 was performed (columns 2 and 3 of Table III). Examples of such a fit are shown in Fig. 4 for different cascades. Then, several spin and multipole mixing ratio hypotheses were tested with an S^2 versus $\arctan(\delta)$ minimization procedure, as described in [24]. In Fig. 5 such an S^2 test is shown for the case of the 959-679 keV cascade. The resulting spin hypotheses that were not rejected and the corresponding multipole mixing ratios for each cascade are shown in columns 4 and 5 of Table III.

B. Level scheme and spin assignment

With the new data, the level scheme of ^{116}Te was extended. A level scheme is displayed in Fig. 7 showing only excited states and transitions observed in this study.

TABLE III. Results of the angular correlation analysis of transitions in coincidence with the $2_1^+ \to 0_1^+$ transition (679 keV).

γ [keV]	a_2	a_4	$J_1 \to J_2 \to J_3$	δ
381	0.44(10)	1.02(10)	$0 \to 2 \to 0$	–
540	$-0.13(3)$	0.26(3)	$2 \to 2 \to 0$	$5.0^{+1.0}_{-0.8}$
959	0.51(5)	0.13(6)	$2 \to 2 \to 0$	$-0.7(1)$
1132	0.1(2)	0.0(2)	$(1, 2, 3, 4) \to 2 \to 0$	–
1402	0.38(6)	1.15(6)	$0 \to 2 \to 0$	–
1587	0.35(5)	$-0.03(12)$	$2 \to 2 \to 0$	$-0.15(15)$
1759	0.1(2)	$-0.3(2)$	$(1, 2, 3, 4) \to 2 \to 0$	–
1830	0.5(2)	0.5(2)	$(0, 2) \to 2 \to 0$	–
1902	0.33(8)	$-0.02(10)$	$2 \to 2 \to 0$	$-0.10(15)$
1955	0.1(2)	$-0.4(3)$	$(1, 2, 3, 4) \to 2 \to 0$	–
2058	0.1(1)	0.0(1)	$(1, 2, 3, 4) \to 2 \to 0$	–
2154	0.6(2)	1.2(2)	$0 \to 2 \to 0$	–

1. Levels at 678.9 and 1359.7 keV

The ordering of the two γ rays belonging to the $2_1^+ \to 0_1^+$ and $4_1^+ \to 2_1^+$ transitions is not always consistent in the literature. Most studies [12–15,17] have identified the 679 keV γ ray with the $2_1^+ \to 0_1^+$ transition and the 681 keV γ ray with the $4_1^+ \to 2_1^+$ transition. However, in [16] this ordering is swapped. Both our measurements confirm the majority of measurements that assign the 679 keV line to the $2_1^+ \to 0_1^+$ transition and the 681 keV line to the $4_1^+ \to 2_1^+$ transition.

2. Level at 1060 keV

The decay of this level to the 2_1^+ (381 keV) has been observed by Zimmerman [12] in β decay before. Zimmerman assigns $J^\pi = 0^+$ to this state based on systematics as well as spin and parity analysis and observes a feeding transition (578 keV) from the level at 1637 keV, to which he assigns a 2^+ state. The assignment of 0^+ to the level at 1060 keV remained somewhat disputed, since Lönnroth *et al.* [13] assigned 3^+ to the level at 1637 keV and did not observe a level at 1060 keV. In this study, a level at 1060 keV and feeding from the level at 1637 keV was observed in both reactions. The angular correlations of the 381-679 keV cascade clearly identify this state as an excited 0^+ state (compare Fig. 4).

3. Level at 1219 keV

This level was first identified by Gowdy *et al.* [25] and the assignment of 2^+ to this state is undisputed. The angular correlation measured in this study show that the $2_2^+ \to 2_1^+$ transition (540 keV) is nearly a pure $E2$ transition. A $2_2^+ \to 0_1^+$ transition (1219 keV) has not been observed in any previous experiment and was also not observed in this study. An upper limit of 1% relative to the intensity of the $2_2^+ \to 2_1^+$ transition (540 keV) was established for the branching of the $2_2^+ \to 0_1^+$ transition (1219 keV) based on the observation limit of this experiment.

4. Level at 1637 keV

As mentioned before, the two studies that have observed this level by Zimmerman [12] and Lönnroth *et al.* [13] disagree on the spin assignment. In this study, the two decays of the level at 1637 keV to the 0_2^+ and 2_1^+ states with transition energies of 578 keV and 959 keV were observed in both experiments. The observed branching ratio of 15(3)% to the 0_2^+ state with respect to the transition to the 2_1^+ state is in agreement with the value reported by Zimmerman [12]. Angular correlations of the 959-679 keV cascade show that the level at 1637 keV has spin 2 and that the decay to the 2_1^+ state (959 keV) is a mixed $E2/M1$ transition with a multipole mixing ratio of $\delta = -0.7(1)$ (compare Fig. 4). The S^2 minimization for this cascade is shown in Fig. 5 clearly identifying that this state has spin 2.

5. Levels at 1811 keV and 2340 keV

Before assigning a spin to the level at 1811 keV, it is useful to assign spin and parity to the level at 2340 keV first. In this study, the level at 2340 keV has been observed only in the α-transfer reaction, where the level was only weakly
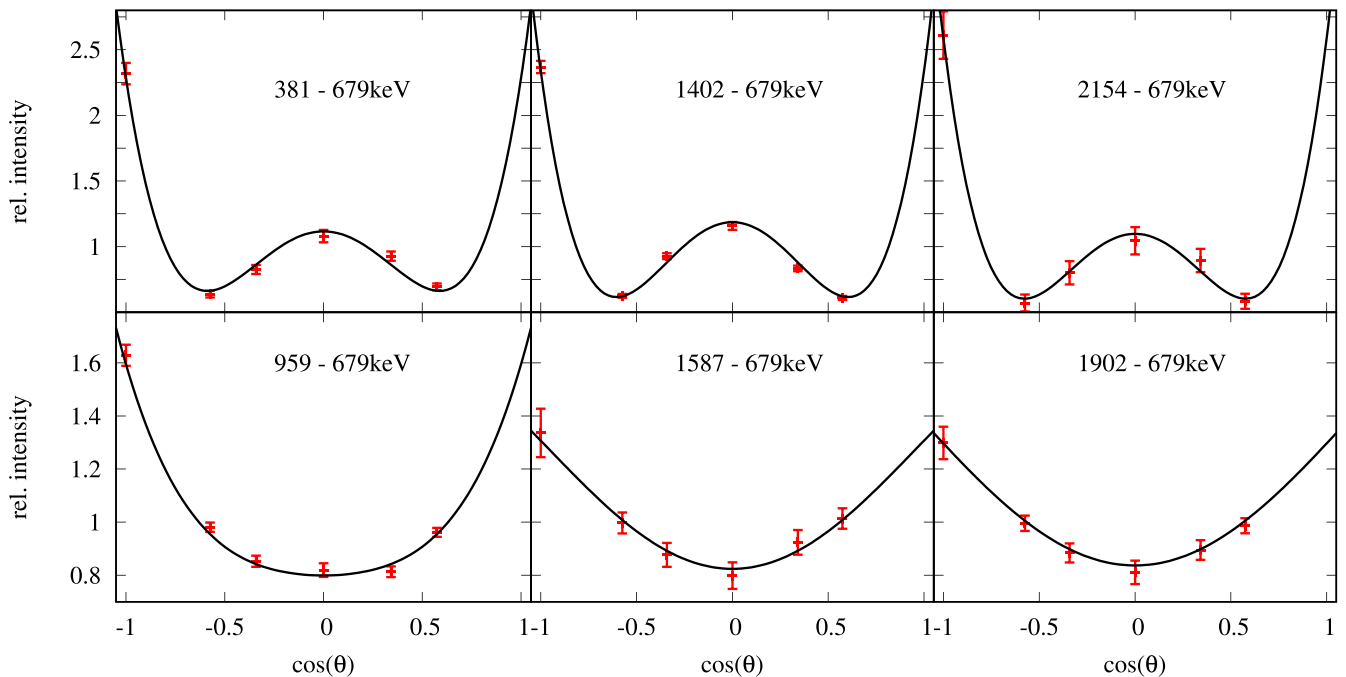
FIG. 4. Angular correlations of γ-γ cascades in ^{116}Te. Experimental intensities are shown in red. The parameters of the best fit, which is shown in black, can be found in Table III.

populated. Decays to the 6_1^+ state and 4_1^+ state were observed. The level was first observed by Lönnroth *et al.* [13] who tentatively assigned spin and parity of 5^+ to the state. More recent studies, however, identify the state at 2340 keV as 6^+ state [15,17] and observe feeding from 8^+ states. Here, this
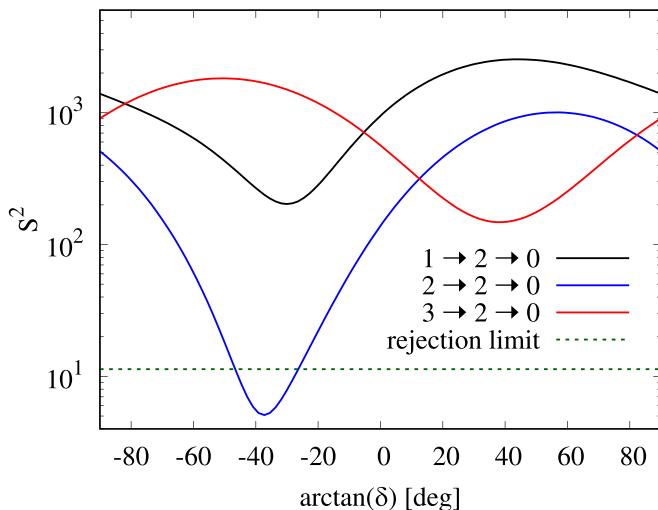

FIG. 5. Spin and multipole mixing ratio determination for the 959-679 keV cascade via angular correlations: For different spin hypotheses of $J_i \rightarrow 2 \rightarrow 0$ cascades, the resulting S^2 minimization is shown depending on the multipole mixing ratio $\delta^2 = \frac{T(L_{\min}+1)}{T(L_{\min})}$. Here, $T(L)$ is the probability to have a transition with angular momentum L. All hypotheses above the 99% confidence limit are rejected and spin 2 is adopted for the 1637 keV state. The multipole mixing ratio is extracted from the minimum S^2 value and the uncertainty is taken at $S_{\min}^2+1$.

latter assignment is adopted. The level at 2340 keV represents thus the 6_2^+ state.

Besides the decays to the 6_1^+ and 4_1^+ state, in two studies [13,15] also a cascade of two transitions with energies of 527 keV and 593 keV was observed connecting the 6_2^+ state at 2340 keV with the 2_2^+ state at 1219 keV. The ordering of these two γ-ray transitions is swapped in the two earlier studies. In [13] the intermediate level is placed at 1811 keV, but in [15] it is placed at 1746 keV. The level at 1811 keV is confirmed by Zimmerman [12] and was also observed in this study in both investigated reactions, but no level at 1746 keV was identified. It is therefore assumed here, that the level at 1746 keV does not exist and that the level at 1811 keV is fed from the level at 2340 keV. This $6_2^+ \rightarrow 4_2^+$ transition was not observed in this study because the statistics were not sufficient. Since the level at 1811 keV has decay branches to the 2_1^+ and 2_2^+ state and is fed from a 6^+ state, here the state is assigned spin and parity of 4^+. In this study, the decays to the 2_2^+ state (1132 keV) and 2_1^+ state (593 keV) were observed in both experiments. The angular correlation of the 1132-679 keV cascade shows no clear anisotropy, but does not contradict a $4 \rightarrow 2 \rightarrow 0$ cascade. It has to be noted though that the branching ratios of the decaying transitions to the 2_1^+ state (1132 keV), 2_2^+ state (593 keV), and 4_1^+ state (452 keV) of this level do not agree for the different reactions (compare Tables I and II). Possible explanations are unobserved contaminations or a level doublet at 1811 keV.

6. Level at 2081 keV

The level has previously been observed by Zimmerman [12] through the decay transitions to the 2_1^+ state (1402 keV) and 2_2^+ state (862 keV) and was assigned spin 1 or 2. But the
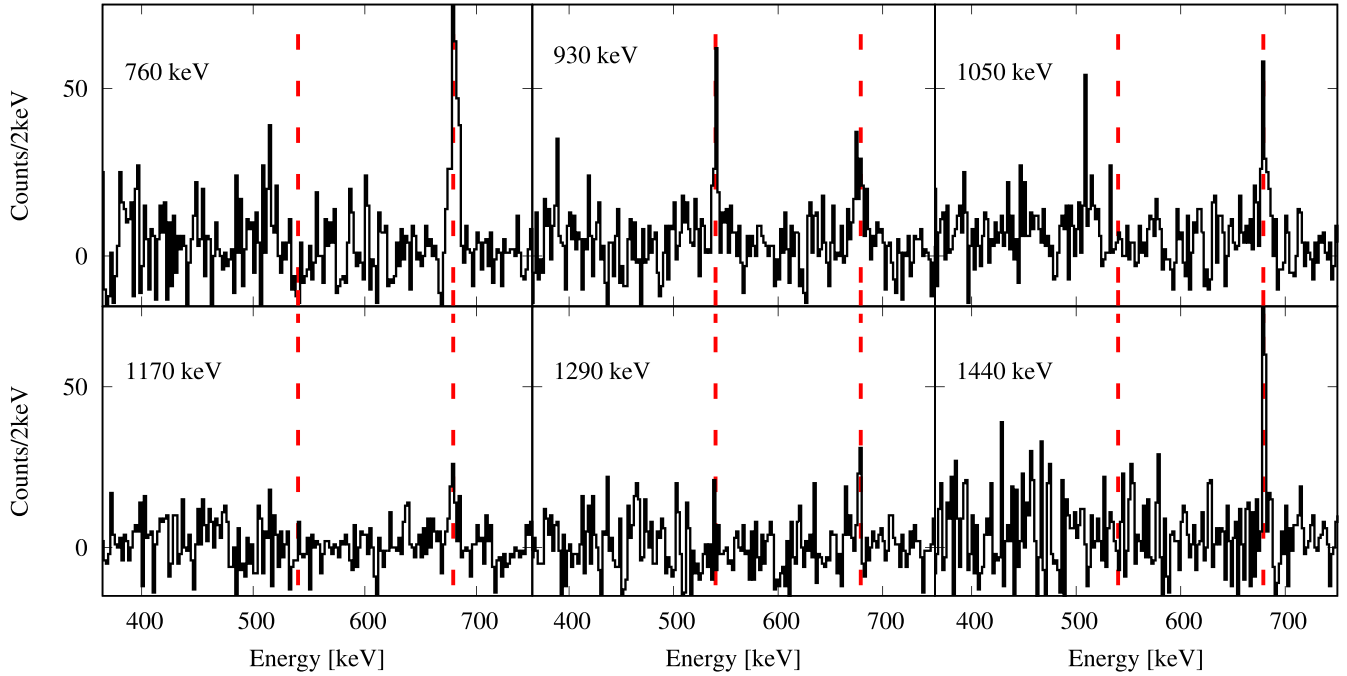
FIG. 6. Doppler corrected spectra obtained from particle-γ-γ coincidences in the α-transfer experiment. The γ gate is set on the transition shown in the upper left corner of each panel, the transition energy is rounded to 10 keV. The particle gate just requires a particle to be detected in the solar cells. The positions of the 680 keV doublet and the $2_2^+ \rightarrow 2_1^+$ transition at 540 keV are marked with red dashed lines. The statistics of all HPGe detectors and all target-to-stopper distances are summed.
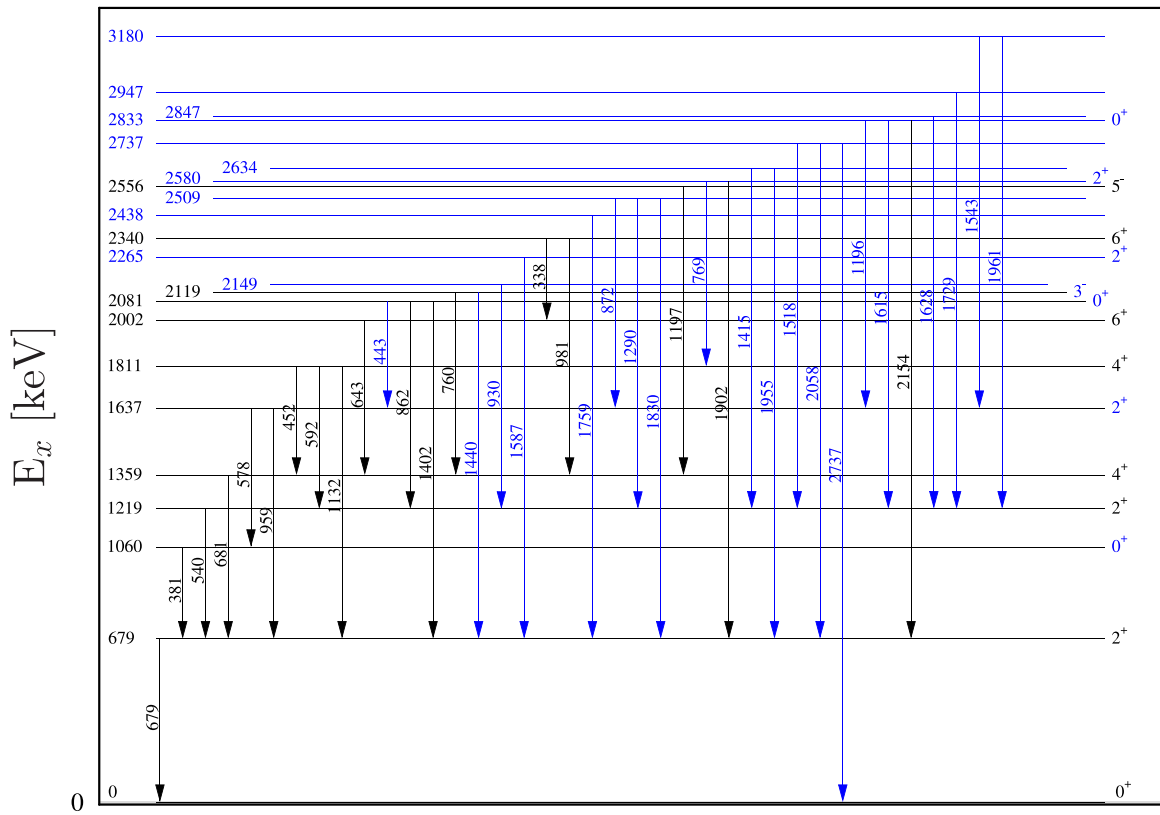
FIG. 7. Level scheme of ^{116}Te observed in the current study. New results are marked with blue color. Blue transitions indicate, that the transition was observed for the first time. Blue level energies and level lines correspond to levels that were placed for the first time. Blue spin and parity imply that the spin and parity were assigned for the first time or clarified. Indentation of lines and numbers is used to improve the readability of the figure.

angular correlation of the 1402-679 keV cascade measured in this study in the β-decay experiment clearly shows that the level at 2081 keV has spin 0 (compare Fig. 4).

7. Level at 2119 keV

This level has been observed by Lönnroth et al. [13] via the 760 keV decay transition to the 4_1^+ state. In the present study, the level was confirmed in the α-transfer experiment. Two decays were observed: the known 760 keV decay to the 4_1^+ state and a previously unknown decay transition (1441 keV) to the 2_1^+ state. The 1441 keV transition matches the energy difference of the level at 2119 keV and the 2_1^+ state and was observed in coincidence with at least one member of the 680 keV doublet in particle-γ-γ coincidences (see Fig. 6). The branching to the 2_1^+ is roughly twice as strong as the previously known decay to the 4_1^+ state. From the spin of the two final states, it is possible to conclude that the level at 2119 keV should have a spin between 2 and 4.

In their study, Lönnroth *et al.* [13] not only measured γ-ray transitions but also conversion electrons and assigned $E1$ to the transition of the level at 2119 keV to the 4_1^+ state (760 keV) with the help of angular distribution coefficients and conversion coefficients. They tentatively assigned 5^- to the state at 2119 keV, but with the present results, a spin of 5 can be excluded and we assign a 3^- to the state.

It is noticeable that the branching ratios of the level at 2119 keV do not resemble branching ratios of the 3_1^- states in neighboring Te isotopes (see [26,27]). To avoid possible assignment errors, further measurements of properties of the state at 2119 keV would be helpful.

8. Level at 2149 keV

In the α-transfer experiment a new transition with an energy of 930 keV was observed. Particle-γ-γ coincidences show coincidences with both 540 keV and 680 keV (compare Fig. 6). A new level is thus placed above the 2_2^+ state at 2149 keV.

9. Level at 2265 keV

This level was observed for the first time in this study. The 1587 keV transition connecting this new state with the 2_1^+ state is observed in both experiments. The angular correlation of the 1587-679 keV cascade suggests that the level has spin 2 and decays with nearly pure $L = 1$ to the 2_1^+ state and was thus assigned a 2^+ (compare Fig. 4).

10. Level at 2509 keV

A level at 2509 keV has not been reported in previous works so far. In this work, three decays to the 2_1^+, 2_2^+, and 2_3^+ with transition energies of 1830 keV, 1290 keV, and 873 keV were identified. The statistics of the angular correlation of the 1830-679 keV cascade are quite poor, but show clear anisotropy. The 1290-540 keV cascade is unfortunately contaminated by random events stemming from the very strong $2_1^+ \rightarrow 0_1^+$ transition in ^{116}Sn and could not therefore be analyzed. The 871-959 keV cascade shows no clear anisotropy.

The anisotropy observed in the 1830-679 keV cascade implies that a spin of 0 and 2 is the most likely.

11. Level at 2580 keV

A transition with an energy of 1902 keV was observed but not placed by Zimmerman [12], since statistics were not sufficient to obtain information from γ-γ coincidences.

In this study, γ-γ coincidences clearly show that the 1902 keV transition is only in coincidence with the 679 keV ground state transition. Angular correlations of the 1902-679 keV cascade are consistent with the level at 2580 keV having spin 2 and the decay to the 2_1^+ state having a nearly pure dipole character (compare Fig. 4). A small branching to the 4^+ state at 1811 keV was identified. The level was also observed in the α-transfer reaction.

12. Level at 2736 keV

This level was observed for the first time in this study in β decay. In γ-γ coincidences, the decays to the 2_1^+ and 2_2^+ state were observed. In the γ-ray singles spectra the decay to the ground state was observed, suggesting that this state has spin 1 or 2.

13. Level at 2832 keV

The 2154 keV transition was observed before by Zimmerman but not placed, because the statistics in γ-γ coincidences was not sufficient. In this study, the 2154 keV transition had observed coincidences with the 679 keV ground state transition only, and a level was thus placed at 2832 keV. The angular correlation shows of the 2154-679 keV cascade measured in this study show, that the level has spin 0 (compare Fig. 4). Additionally, decay branches to the 2_2^+ (1614 keV) and 2_3^+ (1196 keV) states were identified.

14. Levels at 2438 keV, 2634 keV, 2847 keV, 2947 keV, 3180 keV

Levels with these excitation energies were not observed in previous works. The levels were populated only in β decay and were placed with the help of γ-γ coincidences. Angular correlations could not be used to assign a spin to the levels.

15. Transitions with energy 1050 keV, 1171 keV, 1294 keV

These transitions were observed only in the transfer experiment. For all three transitions the Doppler shift corresponded to the kinematics of the ^{112}Sn(^{12}C, ^{8}Be) ^{116}Te α-transfer reaction. Therefore it is very likely that the transitions are indeed transitions in ^{116}Te. In Fig. 6 coincidence spectra are shown. The data suggest that the line at 1050 keV is in coincidence with at least one member of the 680 keV doublet but it was not possible to conclude whether it was in coincidence with just the $2_1^+ \rightarrow 0_1^+$ transition or also the $4_1^+ \rightarrow 2_1^+$ transition. The statistics do not allow to draw a final conclusion on coincident transitions of the 1171 keV and the 1294 keV lines.

C. Lifetime analysis

Lifetimes were measured in the α-transfer experiment using the RDDS method. For a detailed overview of RDDS measurements, the reader is referred to Ref. [18]. In this

experiment, the solar cells registered only protons and α particles stemming from fusion-evaporation reactions as well as α particles stemming from (^{12}C, ^{8}Be) transfer reactions and the subsequent decay of ^{8}Be into two α particles. A gate on higher energies in the solar cells cleared the spectra of fusion evaporation events, as explained at the beginning of Sec. III and only events from the α-transfer reaction remained. Additionally, the energy condition on the solar cells selected events where the target-like nuclei of interest moved with relatively high recoil velocities and more in the beam direction, since the solar cells were mounted at backwards angles.

Data were taken for relative target-to-stopper distances of 1 μm, 8 μm, 18 μm, 30 μm, 70 μm, 120 μm, 200 μm, 300 μm, and 500 μm. The uncertainty of the relative target-to-stopper distances is smaller than 1 μm for small distances and about 1% for distances larger than 100 μm. The absolute distances were determined by extrapolating the dependency of the capacitance on the relative distance. The offset between relative and absolute distances was determined to be 8(5) μm. For details to the capacitance method and the determination of absolute target-to-stopper distances, the reader is referred to Refs. [18,19,28].

The average recoil velocity was determined to be $v/c = 1.1(1)\%$ from the Doppler-shift of transitions populated in the transfer experiment. For the transitions of interest, decay curves $R(x)$ were calculated, where I_s and I_u are the shifted and unshifted components of the transitions of interest, that depend on the distance x:

$$R(x) = \frac{I_u(x)}{I_s(x) + I_u(x)}. \quad (2)$$

Lifetimes τ_i of the level i were analyzed with the differential decay curve method (DDCM) (compare [18]) using the NAPATAU code [29] depending only on precisely known relative target-to-stopper distances and not on the less precisely known absolute distances:

$$\tau_i = \frac{-R_i(x) + \sum_k b_{ki} R_k(x)}{\frac{d}{dx} R_i(x)} \frac{1}{v}. \quad (3)$$

Here, $R_i(x)$ is the decay curve at the distance x for the level i and v is the recoil velocity of the nucleus. The level i is generally fed by several levels k. The factors b_{ki} represent the percentage of the population of the level i that stems from the feeding of the level k. The results of the DDCM analysis were crosschecked with a Monte Carlo approach simulating the Bateman equations as performed in [30]. The Bateman equations,

$$\dot{n}_i(t) = -\lambda_i n_i(t) + \sum_k b_{ki} \lambda_k n_k(t), \quad (4)$$

describe the population $n_i(t)$ of a level i with a lifetime $\tau_i = \frac{1}{\lambda_i}$ with feeding levels k. In the Monte Carlo simulation, the measured lifetimes, initial populations, and intensities of feeding transitions of all feeding levels were varied within the experimental uncertainty in order to simulate the decay curve of the state of interest that then only depends on the lifetime of the state of interest. The results of the simulation can be compared to the experimental data and a best fit for the lifetime can be
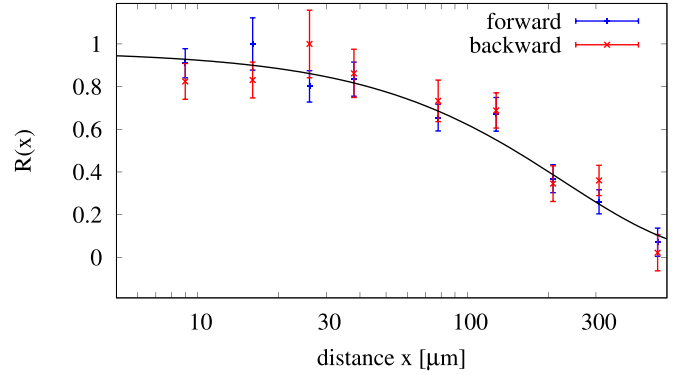

FIG. 8. Decay curve $R(x)$ of the 0_2^+ state for detectors at forward and backward angles depending on absolute distances x. The uncertainty on the absolute distances is not represented in this picture. The uncertainty of the offset is about 5 μm and much larger than the uncertainty of the relative distances which is below 1 μm.

found. In this approach, absolute target-to-stopper distances have to be used.

For the lifetime of the 6_1^+ state, the intensities of the shifted and unshifted components of the $6_1^+ \rightarrow 4_1^+$ transition (643 keV) were determined in particle-gated γ-ray spectra, but uncertainties in the lifetime of the 6_2^+ state, feeding the 6_1^+ state via the observed $6_2^+ \rightarrow 6_1^+$ transition (338 keV) and possible unobserved feeding limited the analysis to give only an upper limit of 8 ps for the lifetime. Also for the 4_2^+ state, only an upper limit of the lifetime could be determined: the discrepancy between the lifetime values obtained using the DDCM and the Monte Carlo simulation of the Bateman equation was too large to give a more reliable value for the lifetime. The lifetime was determined to be smaller than 11 ps.

The lifetimes of the 2_2^+ and 0_2^+ states were analyzed using particle-gated spectra and correcting for the observed feeding from the 4_2^+ state and the 2_3^+ state, respectively, that were determined experimentally. An upper limit of possible unobserved long lived feeding has been estimated by the observation limit and is accounted for in the uncertainty. Due to the direct character of the α-transfer reaction it is however not likely that unobserved long lived feeding plays a larger role. The development of the decay curve of the 0_2^+ state depending on the target-to-stopper distance is shown in Fig. 8.

The lifetime of the 2_1^+ state was measured using particle-γ-γ coincidences and a full gate on both components of the $2_2^+ \rightarrow 2_1^+$ (540 keV) transition. This avoids the complications arising from the analysis of the doublet at 680 keV. Furthermore it excludes the possibility of unobserved long lived feeding but also greatly reduces the statistics, that now become the main contribution to the uncertainty. The lifetime was determined to be 5(2) ps. In Fig. 9 spectra are shown, that demonstrate how the ratio of shifted and unshifted components develops with increasing distance.

With a value for the lifetime of the 2_1^+ it was possible to give an estimation for the lifetime of the 4_1^+ state analyzing the 680 keV doublet. The separation between the $4_1^+ \rightarrow 2_1^+$ and $2_1^+ \rightarrow 0_1^+$ transitions is far smaller than the separation between the respective Doppler-shifted and unshifted
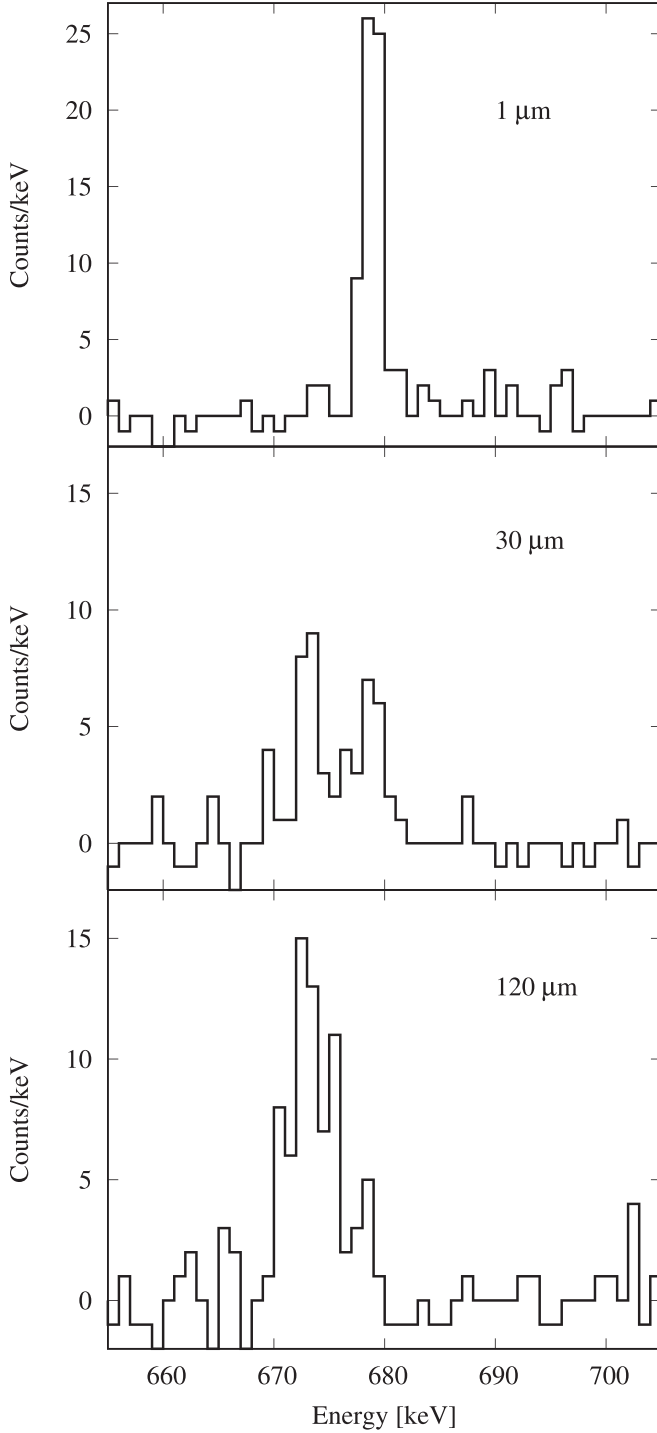
FIG. 9. Spectra of the $2_1^+ \rightarrow 0_1^+$ transition for different relative target-to-stopper distances from detectors at backward angles. A full gate on both components was set on the $2_2^+ \rightarrow 2_1^+$ (540 keV) transition and a solar cell condition. Since the spectra are not Doppler-corrected, the shifted component is significantly broader than the unshifted component.

TABLE IV. Lifetime values of the results of the DDCM and Monte Carlo Bateman analysis. The upper limits vary with the observed intensities of the decaying transitions. The results of the two analysis methods are not independent. If a DDCM analysis was possible, the result of the DDCM is used and only crosschecked with the Monte Carlo simulation. The adopted values are indicated. Note that the transitions with energies 1050, 1171 and 1294 keV could not be placed in the level scheme and hence do not appear in Fig. 7.

J_i^π or E_γ	τ (DDCM) [ps]	τ (Bateman) [ps]	Adopted [ps]
2_1^+	5(2)	7(4)	5(2)
0_2^+	69(9)	69(11)	69(9)
2_2^+	12.3(15)	12(2)	12.3(15)
4_1^+		$1 < \tau < 9$	$1 < \tau < 9$
2_3^+		<2	<2
4_2^+	7(2)	4(2)	<11
6_1^+		<8	<8
5_1^-		<10	<10
930		<10	<10
1050		<10	<10
1171		<10	<10
1294		<20	<20
3_1^-		<5	<5
2_4^+		<10	<10
2_5^+		<10	<10

simulation of the Bateman equations together with the known value of the lifetime of the 2_1^+ state to determine the lifetime of the 4_1^+ state. A lower limit of 1 ps and an upper limit of 9 ps were determined for the lifetime of the 4_1^+ state. The value for the lifetime of the 4_1^+ correlates with the value of the lifetime of the 2_1^+ state.

For the remaining states it was only possible to determine upper limits of the lifetimes since they were shorter than the lifetimes measurable in this experiment. The measured lifetimes are summarized in Table IV.

With the new spin assignments, branching ratios, lifetimes, and multipole mixing ratios, absolute transition strengths can be calculated. All experimental findings are summarized in Table V.

IV. DISCUSSION

A level scheme of ^{116}Te using the new experimental data from this study is shown in Fig. 7. Experimental level energies and $B(E2)$ values suggest, that the 0_2^+, 2_2^+, and 4_1^+ states are suitable candidates for a two-phonon triplet within the U(5) limit of the IBM-1 model [34] (compare Fig. 10). A calculation has been performed using the general U(5) Hamiltonian [35]

$$\mathbf{H} = \epsilon \mathbf{n_d} + \alpha \mathbf{n_d}(\mathbf{n_d} + 4) + \beta\left(\tfrac{1}{5}\mathbf{LL} + 2\mathbf{T_3T_3}\right) + \gamma \mathbf{LL} \quad (5)$$

with the parameters $\varepsilon = 0.62$ MeV, $\alpha = -0.015$ MeV, $\beta = 0.011$ MeV, $\gamma = 0.009$ MeV, and e_B=10.35 $e$fm^2 a reasonable agreement of experimental data and IBM-1 prediction was found. The calculations were performed with the ARBMODEL code [36]. Figure 10 shows a comparison of experimental level energies and $B(E2)$ values with results of the calculation. In general, both level ordering and $B(E2)$ values from the

components so that it was possible to reliably determine the summed intensity of the shifted components of both transitions and the summed intensity of the unshifted components of both transitions. These were used to perform a Monte Carlo

TABLE V. All observed experimental values in ^{116}Te in this study. The branching ratios relatively to the strongest observed decay are given in column "b", β stands for populated in β decay and t stands for populated in transfer reaction.

E_{level} [keV]	J_i^π	E_γ [keV]	E_f [keV]	J_f^π	b	τ [ps]	EL	δ	$B(EL)$ [W.u.]	Reaction
678.8(1)	2_1^+	678.8(1)	0.0	0_1^+	100	5(2)	$E2$		33_{-10}^{+22}	β,t
1059.7(1)	0_2^+	380.9(1)	678.8	2_1^+	100	69(9)	$E2$		43_{-5}^{+6}	β,t
1218.7(1)	2_2^+	539.9(1)	678.8	2_1^+	100	12.3(15)	$E2$	$5.2_{-0.8}^{+1.0}$	41_{-5}^{+6}	β,t
							$M1$		$6_{-2}^{+4} \times 10^{-4}$	
1359.4(3)	4_1^+	680.6(3)	678.8	2_1^+	100	$1 < \tau < 9$	$E2$		$20 < B(E2) < 170$	β,t
1637.3(2)	2_3^+	419	1218.7	2_2^+	< 3	< 2	$M1+E2$			β
		577.6(1)	1059.7	0_2^+	15(3)		$E2$		> 20	β,t
		958.5(2)	678.8	2_1^+	100(2)		$E2$	$-0.7_{-0.1}^{+0.1}$	> 3	β,t
							$M1$		>0.01	
1811.2(3)	4_2^+	452	1359.4	4_1^+	14(3)	<11	$M1+E2$			β,t
		592.5(2)	1218.7	2_2^+	35(15)		$E2$		>5	β,t
		1132.4(3)	678.8	2_1^+	100(3)		$E2$		>0.7	β,t
2002.2[a]	6_1^+	643.1[a]	1359.4	4_1^+	100	< 8	$E2$		>27	t
2080.5(2)	0_3^+	443.3	1637.3	2_3^+	< 7		$E2$			β
		861.8(1)	1218.7	2_2^+	49(5)		$E2$			β
		1401.7(4)	678.8	2_1^+	100(7)		$E2$			β
2119.1[a]	3_1^- [c]	759.7[b]	1359.4	4_1^+	47(7)	< 5	$E1$[bc]		$>5 \times 10^{-5}$	t
		1441(2)	678.8	2_1^+	100(7)		$E1$[c]		$>1.8 \times 10^{-5}$	t
2149(2)		930(2)	1218.7	2_2^+	100	<10				t
2265.6(5)	2_4^+	1586.8(5)	678.8	2_1^+	100	<10	$M1(+E2)$	$-0.15(15)$	$>7 \times 10^{-4}$	β,t
2339.9[a]	6_2^+	337.9[a]	2002.2	6_1^+	100(11)		$M1+E2$			t
		980.5[a]	1359.4	4_1^+	83(11)		$E2$			t
2438.2(7)		1759.4(7)	678.8	2_1^+	100					β
2508.6(3)		871.3(2)	1637.3	2_3^+	39(4)		$E2$			β
		1290.0(5)	1218.7	2_2^+	100(15)		$E2$			β
		1829.9(6)	678.8	2_1^+	18(2)		$E2$			β
2556.1[a]	5_1^- [b]	1196.7[b]	1359.4	4_1^+	100	<10	$E1$[b]			t
2580.4(4)	2_5^+	769(1)	1811.2	4_2^+	11(6)	<10	$E2$		>0.8	β
		1901.6(4)	678.8	2_1^+	100(11)		$M1(+E2)$	$-0.10(15)$	$>4 \times 10^{-4}$	β,t
2633.4(4)		1414.7(4)	1218.7	2_2^+	43(5)					β
		1954.7(5)	678.8	2_1^+	100(10)					β
2736.5(5)		1517.9(4)	1218.7	2_2^+	100(7)					β
		2057.7(5)	678.8	2_1^+	66(7)					β
		2736(1)	0.0	0_1^+	71(14)					β
2832.8(5)	0_4^+	1195.6(4)	1637.3	2_3^+	42(5)		$E2$			β
		1614.1(5)	1218.7	2_2^+	78(8)		$E2$			β
		2153.8(6)	678.8	2_1^+	100(17)		$E2$			β
2846.7(5)		1628.0(5)	1218.7	2_2^+	100					β
2947.4(6)		1728.7(6)	1218.7	2_2^+	100					β
3179.1(5)		1542.7(5)	1637.3	2_3^+	54(6)					β
		1961.4(4)	1218.7	2_2^+	100(16)					β
unplaced transitions:										
		1050(2)				<10				t
		1171(2)				<10				t
		1294(2)				<20				t

[a] Adopted from [11].

[b] Adopted from [13].

[c] The assignment of 3^- to the level at 2119 keV and the subsequent assignment of E1 to the decay transition to the 2_1^+ state are based on the assignment of E1 to the 760 keV transition by Lönnroth et al. [13]. See text for details.

IBM-1 calculations agree with the experimental values. The most prominent differences are the missing of a candidate for the 3^+ state of the three phonon quintuplet and the placement of the 0_3^+ state. It is however possible, that the correct candidates for the three phonon quintuplet have not been identified yet. Another difference is the decay pattern of the 2_3^+. The $B(E2, 2_3^+ \rightarrow 2_1^+)$ was measured to be larger than three W.u. in this study, but this transition is forbidden in the IBM-1.

So far, the 0_2^+ was treated as a member of the two phonon triplet of the U(5) limit of the IBM-1. A second possible
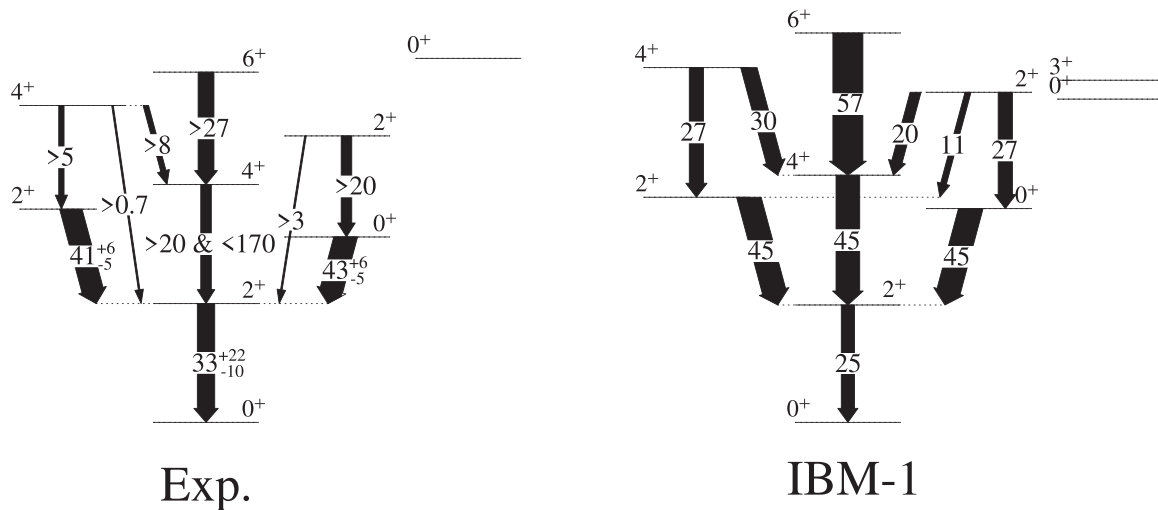
FIG. 10. Comparison of the IBM-1 calculation with the experimental results. $B(E2)$ strengths are given in W.u. For simplicity, for the experimental data the $4_2^+ \rightarrow 4_1^+$ transition is assumed to be a pure $E2$ transition as no multipole mixing ratio was determined.

explanation for the low-lying 0_2^+ state can be intruder states from 4p-2h excitations across the $Z = 50$ proton shell closure. Such intruder states have been suggested in some cases in the Te isotopes (compare, e.g., [1]) but have not been identified unambiguously yet. The strongly collective $E2$ transition from the 2_3^+ state to the 0_2^+ state can be interpreted as the beginning of a band structure on top of the 0_2^+. Further supporting arguments for an intruder structure are the energy systematics of the 0_2^+ and 2_3^+ states in the Te isotopes that show a parabolic behavior with a minimum at midshell ^{118}Te (compare Fig. 11). This behavior has been observed already by Rikovska *et al.* [7] and this study extends the picture by clearly identifying the spin of the candidate states for the intruding 0_2^+ and 2_3^+ state. If the 0_2^+ state is interpreted as a state belonging to an intruding structure, a suiting candidate for a 0_2^+ state belonging to the two phonon triplet of the structure of the ground state is missing.
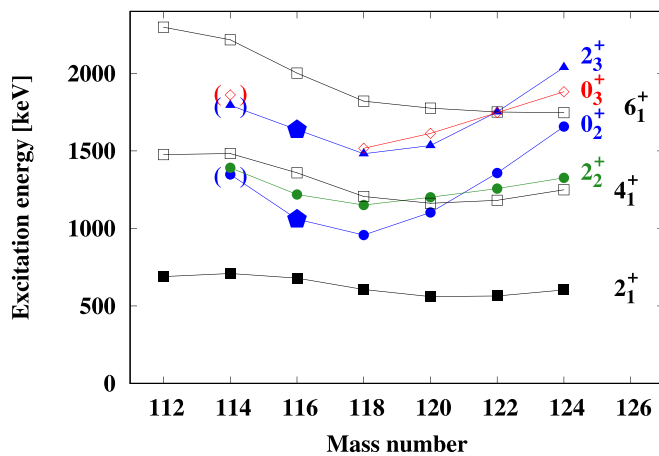

FIG. 11. Systematics of low-lying levels in midshell Te isotopes [11,26,27,31–33]. States where the spin and parity assignment could be improved in this study are marked with a ⬦ symbol. Several states in ^{114}Te are marked in brackets since the spin assignment is tentative.

Both approaches—a description completely within the U(5) limit and the introduction of shape coexistence—provide a sufficient explanation of the experimental data. To further test both hypotheses, more experimental data are needed. For example, other reaction mechanisms could be able to identify suited candidates for the 3^+ and 0^+ member of the three-phonon quintuplet in the U(5) approach. The systematics of the 0_3^+ state along the Te isotopic chain do indeed suggest, that a 0^+ state is missing in ^{116}Te at around 1.5–1.7 MeV (compare Fig. 11). The $B(E2)$ values of transitions in the yrast band were determined in this study only with relatively large uncertainties. More precise values could therefore help to further test the predictions of a description within the U(5) limit.

An enhanced $\rho(E0)$ value of the $0_2^+ \rightarrow 0_1^+$ transition is often an indicator for different shapes of the respective 0^+ states and depends on the mixing of those states [1]. The direct $E0$ transition from the 0_2^+ to the ground state has, however, not been measured yet. More spectroscopy is needed to establish a possible band structure on top of the 0_2^+ state. A candidate for an intruding 4^+ state is missing and hence also the needed in-band decays of the intruding structure. The (^{3}He, n) reactions are also known to strongly populate intruder states [1]. A measurement of the relative cross sections of the direct population of the 0_1^+ and 0_2^+ states is another possible indicator for shape coexistence.

The role that (^{12}C, ^{8}Be) α-transfer reactions play at investigating nuclear structure has not fully been understood so far. Stahl *et al.* [37] find that the ^{12}C(^{136}Xe, ^{140}Ba) ^{8}Be reaction strongly populates the 2_{ms}^+ mixed-symmetry state, though not as strong as predicted by Alonso *et al.* [38]. In this study, the 2_4^+ and 2_5^+ states were populated in the α-transfer reaction and both decay with nearly pure $M1$ transitions to the 2_1^+ state. However, for none of these states a transition to the ground state has been found and the absolute $M1$ strengths are unknown since only an upper limit for the lifetimes was established.

Astier *et al.* [39,40] find that the α-transfer reaction ^{208}Pb(^{18}O, ^{14}C)^{212}Po populates states that can be identified to belong to α clustering structures. They manifest through strong $E1$ transitions to states with the same spin but different parity. Candidates for such states could be the newly discovered states in the transfer reaction in this study, but for many of them, it was not possible to assign multipolarities to the decaying transitions and to determine their spin and parity. Astier also observed a strong population of the 3_1^- state, which could also be observed in this experiment.

V. CONCLUSION

The level structure of low-lying and low spin states in ^{116}Te has been investigated. Several new states were found.

Spins and multipole mixing ratios were measured with the help of angular correlations. Absolute transition strengths of low-lying states have been calculated using lifetimes measured in an RDDS experiment. The resulting data allow an interpretation of the nucleus in the U(5) limit of the IBM-1 but do not contradict the possibility of shape coexistence. To clarify the picture, more experimental data are needed.

[1] P. E. Garrett, M. Zielińska, and E. Clément, An experimental view on shape coexistence in nuclei, Prog. Part. Nucl. Phys. **124**, 103931 (2022).

[2] B. L. Cohen and R. E. Price, Studies of low-lying levels of even-even nuclei with (d, p) and (d, t) reactions, Phys. Rev. **118**, 1582 (1960).

[3] H. Fielding, R. Anderson, C. Zafiratos, D. Lind, F. Cecil, H. Wieman, and W. Alford, 0^+ states observed in Cd and Sn nuclei with the (^{3}He, n) reaction, Nucl. Phys. A **281**, 389 (1977).

[4] R. A. Meyer and L. Peker, Evidence for the coexistence of shapes in even-mass Cd nuclei, Z. Phys. A At. Nucl. **283**, 379 (1977).

[5] P. E. Garrett, T. R. Rodríguez, A. Diaz Varela, K. L. Green, J. Bangay, A. Finlay, R. A. E. Austin, G. C. Ball, D. S. Bandyopadhyay, V. Bildstein, S. Colosimo, D. S. Cross, G. A. Demand, P. Finlay, A. B. Garnsworthy, G. F. Grinyer, G. Hackman, B. Jigmeddorj, J. Jolie, W. D. Kulp *et al.*, Shape coexistence and multiparticle-multihole structures in ^{110,112}Cd, Phys. Rev. C **101**, 044302 (2020).

[6] J. L. Wood, K. Heyde, W. Nazarewicz, M. Huyse, and P. van Duppen, Coexistence in even-mass nuclei, Phys. Rep. **215**, 101 (1992).

[7] J. Rikovska, N. J. Stone, P. M. Walker, and W. B. Walters, Intruder states in even-even Te nuclei, Nucl. Phys. A **505**, 145 (1989).

[8] A. A. Pasternak, J. Srebrny, A. D. Efimov, V. M. Mikhajlov, E. O. Podsvirova, C. Droste, T. Morek, S. Juutinen, G. B. Hagemann, M. Piiparinen, S. Törmänen, and A. Virtanen, Lifetimes in the ground-state band and the structure of ^{118}Te, Euro. Phys. J. A **13**, 435 (2002).

[9] O. Möller, N. Warr, J. Jolie, A. Dewald, A. Fitzler, A. Linnemann, K. O. Zell, P. E. Garrett, and S. W. Yates, E2 transition probabilities in ^{114}Te: A conundrum, Phys. Rev. C **71**, 064324 (2005).

[10] C. Mihai, A. A. Pasternak, S. Pascu, D. Filipescu, M. Ivaşcu, D. Bucurescu, G. Căta Danil, I. Căta-Danil, D. Deleanu, D. G. Ghiţă, T. Glodariu, N. Mărginean, R. Mărginean, A. Negret, T. Sava, L. Stroe, G. Suliman, and N. V. Zamfir, Lifetime measurements by the Doppler-shift attenuation method in the ^{115}Sn($\alpha, n\gamma$)^{118}Te reaction, Phys. Rev. C **83**, 054310 (2011).

[11] J. Blachot, Nuclear Data Sheets for A = 116, Nucl. Data Sheets **111**, 717 (2010).

[12] B. E. Zimmerman, The energy level structures of even-even tellurium and odd-odd iodine and antimony nuclei: ^{114}Te, ^{116}Te, ^{114}I, and ^{114}Sb, Ph.D. thesis, University of Maryland (1992).

[13] T. Lönnroth, A. Virtanen, and J. Hattula, Coexistence of vibrational and quasiparticle structures in neutron-deficient ^{114,115,116,117}Te, Phys. Scr. **34**, 682 (1986).

[14] P. Chowdhury, W. F. Piel, and D. B. Fossan, Collective properties of $1g_{\frac{9}{2}}$ proton-hole excitations: High-spin states in ^{116,118,120,122}Te and ^{120}Xe nuclei, Phys. Rev. C **25**, 813 (1982).

[15] A. Sharma, J. Singh, H. Kaur, J. Goswamy, D. Mehta, N. Singh, P. N. Trehan, E. S. Paul, and R. K. Bhowmik, High spin states in ^{116,118}Te, Z. Phys. A Hadrons and Nuclei **354**, 347 (1996).

[16] J. M. Sears, D. B. Fossan, I. Thorslund, P. Vaska, E. S. Paul, K. Hauschild, I. M. Hibbert, R. Wadsworth, S. M. Mullins, A. V. Afanasjev, and I. Ragnarsson, High-spin spectroscopy of $^{116}_{52}$Te, Phys. Rev. C **55**, 2290 (1997).

[17] C. B. Moon, T. Komatsubara, T. Shizuma, K. Uchiyama, N. Hashimoto, M. Katoh, K. Matsuura, M. Murasaki, Y. Sasaki, H. Takahashi, Y. Tokita, and K. Furuno, In-beam gamma-ray spectroscopy of ^{116}Te, Z. Phys. A Hadrons and Nuclei **358**, 373 (1997).

[18] A. Dewald, O. Möller, and P. Petkov, Developing the recoil distance doppler-shift technique towards a versatile tool for lifetime measurements of excited nuclear states, Prog. Part. Nucl. Phys. **67**, 786 (2012).

[19] T. Alexander and A. Bell, A target chamber for recoil-distance lifetime measurements, Nucl. Instrum. Methods **81**, 22 (1970).

[20] L. Netterdon, V. Derya, J. Endres, C. Fransen, A. Hennig, J. Mayer, C. Müller-Gatermann, A. Sauerwein, P. Scholz, M. Spieker, and A. Zilges, The γ-ray spectrometer HORUS and its applications for nuclear astrophysics, Nucl. Instrum. Methods Phys. Res. A **754**, 94 (2014).

[21] J. K. Smith, A. D. MacLean, W. Ashfield, A. Chester, A. B. Garnsworthy, and C. E. Svensson, Gamma–gamma angular correlation analysis techniques with the Griffin spectrometer, Nucl. Instrum. Methods Phys. Res. A **922**, 47 (2019).

[22] L. Knafla, A. Esmaylzadeh, A. Harter, J. Jolie, U. Köster, M. Ley, C. Michelagnoli, and J.-M. Régis, Development of a new $\gamma-\gamma$ angular correlation analysis method using a symmetric

ring of clover detectors, Nucl. Instrum. Methods Phys. Res. A **1042**, 167463 (2022).

[23] H. J. Rose and D. M. Brink, Angular distributions of gamma rays in terms of phase-defined reduced matrix elements, Rev. Mod. Phys. **39**, 306 (1967).

[24] S. Robinson, How reliable are spins and δ-values derived from directional correlation experiments? Nucl. Instrum. Methods Phys. Res. A **292**, 386 (1990).

[25] G. M. Gowdy, A. C. Xenoulis, J. L. Wood, K. R. Baker, R. W. Fink, J. L. Weil, B. D. Kern, K. J. Hofstetter, E. H. Spejewski, R. L. Mlekodaj, H. K. Carter, W. D. Schmidt-Ott, J. Lin, C. R. Bingham, L. L. Riedinger, E. F. Zganjar, K. S. R. Sastry, A. V. Ramayya, and J. H. Hamilton, On-line mass separator investigation of the new isotope 2.9-sec ^{116}I, Phys. Rev. C **13**, 1601 (1976).

[26] K. Kitao, Nuclear Data Sheets for A = 118, Nucl. Data Sheets **75**, 99 (1995).

[27] K. Kitao, Y. Tendow, and A. Hashizume, Nuclear Data Sheets for A = 120, Nucl. Data Sheets **96**, 241 (2002).

[28] M. Beckers, A. Dewald, C. Fransen, L. Kornwebel, C.-D. Lakenbrink, and F. von Spee, Revisiting the measurement of absolute foil-separation for RDDS measurements and introduction of an optical measurement method, Nucl. Instrum. Methods Phys. Res. A **1042**, 167416 (2022).

[29] B. Saha, Bestimmung der Lebensdauern kollektiver Kernanregungen in ^{124}Xe und Entwicklung von entsprechender Analysesoftware, Ph.D. thesis, Universität zu Köln (2004).

[30] A. Esmaylzadeh, V. Karayonchev, K. Nomura, J. Jolie, M. Beckers, A. Blazhev, A. Dewald, C. Fransen, R.-B. Gerst, G. Häfner, A. Harter, L. Knafla, M. Ley, L. M. Robledo, R. Rodríguez-Guzmán, and M. Rudigier, Lifetime measurements to investigate γ softness and shape coexistence in ^{102}Mo, Phys. Rev. C **104**, 064314 (2021).

[31] J. Blachot, Nuclear Data Sheets for A = 114, Nucl. Data Sheets **113**, 515 (2012).

[32] T. Tamura, Nuclear Data Sheets for A = 122, Nucl. Data Sheets **108**, 455 (2007).

[33] J. Katakura and Z. Wu, Nuclear Data Sheets for A = 124, Nucl. Data Sheets **109**, 1655 (2008).

[34] A. Arima and F. Iachello, Interacting boson model of collective states I. The vibrational limit, Ann. Phys. **99**, 253 (1976).

[35] F. Iachello and A. Arima, *The Interacting Boson Model*, Cambridge Monographs on Mathematical Physics (Cambridge University Press, Cambridge, UK, 1987).

[36] S. Heinze, Eine Methode zur Lösung beliebiger bosonischer und fermionischer Vielteilchensysteme, Ph.D. thesis, Universität zu Köln (2008).

[37] C. Stahl, J. Leske, C. Bauer, D. Bazzacco, E. Farnea, A. Gottardo, P. R. John, C. Michelagnoli, N. Pietralla, M. Reese, E. Şahin, B. Birkenbach, A. Bracco, F. C. L. Crespi, G. de Angelis, P. Désesquelles, J. Eberth, A. Gadea, A. Görgen, J. Grebosz *et al.*, Population of the 2^+_{ms} mixed-symmetry state of ^{140}Ba with the α-transfer reaction, Phys. Rev. C **92**, 044324 (2015).

[38] C. E. Alonso, J. M. Arias, L. Fortunato, N. Pietralla, and A. Vitturi, Population of mixed-symmetry states via α transfer reactions, Phys. Rev. C **78**, 017301 (2008).

[39] A. Astier, P. Petkov, M.-G. Porquet, D. S. Delion, and P. Schuck, Novel manifestation of α-clustering structures: New "$\alpha + {}^{208}$Pb" states in ^{212}Po revealed by their enhanced $E1$ decays, Phys. Rev. Lett. **104**, 042701 (2010).

[40] A. Astier, P. Petkov, M.-G. Porquet, D. S. Delion, and P. Schuck, Coexistence of "$\alpha + {}^{208}$Pb" cluster structures and single-particle excitations in $^{212}_{84}$Po$_{128}$, Eur. Phys. J. A **46**, 165 (2010).